

## Studies of irradiated two-phase lithium ceramics $\text{Li}_4\text{SiO}_4/\text{Li}_2\text{TiO}_3$ by thermal desorption spectroscopy

Yevgen Chikhray<sup>a</sup>, Saulet Askerbekov<sup>a,b,\*</sup>, Regina Knitter<sup>c</sup>, Timur Kulsartov<sup>a,d</sup>, Asset Shaimerdenov<sup>b</sup>, Magzhan Aitkulov<sup>b</sup>, Assyl Akhanov<sup>b</sup>, Darkhan Sairanbayev<sup>b</sup>, Zhanar Bugybay<sup>b</sup>, Aigerim Nessipbay<sup>b</sup>, Kirill Kisselyov<sup>b</sup>, Gunta Kizane<sup>e</sup>, Arturs Zarins<sup>e</sup>

<sup>a</sup> al-Farabi Kazakh National University, Almaty, Kazakhstan

<sup>b</sup> Institute of Nuclear Physics, Almaty, Kazakhstan

<sup>c</sup> Karlsruhe Institute of Technology, Karlsruhe, Germany

<sup>d</sup> Kazakh-British Technical University, Almaty, Kazakhstan

<sup>e</sup> University of Latvia, Riga, Latvia

### ARTICLE INFO

#### Keywords:

Two-phase lithium ceramics  
Tritium  
Neutron irradiation  
Tritium release  
TDS  
RGA

### ABSTRACT

Two-phase ceramics  $\text{Li}_2\text{TiO}_3\text{-Li}_4\text{SiO}_4$  are one of the potentially promising materials for creating a ceramic blanket for DEMO reactor. However, until now, a limited number of studies have been carried out on the release of tritium from this material under the influence of neutron irradiation, which poses fundamental problems for its application.

In this work, the pebbles of two-phase lithium ceramics consisting of 25 mol%  $\text{Li}_2\text{TiO}_3$  and 75 mol%  $\text{Li}_4\text{SiO}_4$  were studied using thermal desorption spectroscopy (TDS) after their irradiation with neutrons at the WWR-K research reactor. Under the conditions of the irradiation experiment, which lasted 21.5 days at a reactor power of 6 MW, the samples were exposed to thermal neutrons with a flux density of  $2 \cdot 10^{13} \text{ n}/(\text{cm}^2 \times \text{s})$ . The thermal neutron fluence accumulated as a result of irradiation was  $3.7 \cdot 10^{19} \text{ cm}^{-2}$ .

It has been established that tritium comes out mainly in the form of HT molecules and has three visible TDS peaks, which can be described by three rates of the first-order desorption reaction with an activation energy of 90 kJ/mol. Experiments have shown that the main amount of tritium is evenly distributed throughout the pebble's pores and voids. Its yield is determined by desorption and transfer from inner voids to the boundaries that communicate with the outer surface of the sample. The kinetics of tritium release depends on the number, size and depth of the exit paths of such areas inside the ceramic.

### Introduction

Fusion reactors operating on the basis of the D-T (deuterium–tritium) reaction represent a promising direction in the field of clean energy production. However, for such reactors to operate efficiently, it is necessary to generate and retain tritium (T), which serves as one of the fuel materials. Tritium breeding materials play a key role in this process, and one of the potentially promising materials for creating ceramic blankets is  $\text{Li}_2\text{TiO}_3\text{-Li}_4\text{SiO}_4$  two-phase ceramics [1–4]. To date, numerous reactor studies on two-phase lithium ceramics have been conducted [5–7], including the authors of this article [8,9]. It should be noted here that the authors studied this ceramic in situ experiments both within the framework of international projects [10] and national

scientific programs of the Republic of Kazakhstan [11–13], devoted to problems in broad areas of nuclear and fusion energy: from issues of radioecology to plasma experiments on the tokamak KTM [14–21]. These studies have demonstrated that a deep understanding of tritium retention and release processes relies significantly on knowledge of structural changes and surface morphology of the specimens. However, handling a large number of specimens can present certain challenges. The uniqueness of this study lies in its provision of thermal desorption spectroscopy (TDS) results for an individual pebble, significantly broadening our comprehension of these processes.

As our experiments and those of other authors [22–25] have shown, there are a number of radiation-stimulated processes that significantly affect the structure and, consequently, the processes of gas transfer in

\* Corresponding author.

E-mail address: [askerbekov@physics.kz](mailto:askerbekov@physics.kz) (S. Askerbekov).

<https://doi.org/10.1016/j.nme.2024.101621>

Received 10 November 2023; Received in revised form 14 February 2024; Accepted 19 February 2024

Available online 23 February 2024

2352-1791/© 2024 The Author(s). Published by Elsevier Ltd. This is an open access article under the CC BY-NC license (<http://creativecommons.org/licenses/by-nc/4.0/>).

materials. As for the direct study of irradiated two-phase lithium ceramics by other authors [26,27,4,6,7], they were also carried out mainly by the TDS method, which allowed us to determine a number of parameters of tritium release. The studies presented in this article were performed with samples irradiated to significantly higher neutron fluencies than in the above-mentioned works and may be interesting from the point of view of the development of the concept of the mechanisms of interaction of tritium with lithium ceramics.

The objective of this study was to determine the mechanisms and features of the release of tritium produced in two-phase ceramics 25 % LMT + 75 %LOS using the TDS method. The results obtained may be important for the further development and optimization of ceramic blankets in fusion reactors and ensuring their safe and efficient operation.

### Samples studied

In this work, samples of two-phase lithium ceramics consisting of 25 mol%  $\text{Li}_2\text{TiO}_3$  and 75 mol%  $\text{Li}_4\text{SiO}_4$  (denoted as 25 %LMT + 75 %LOS), which were subjected to neutron irradiation at the WWR-K reactor in Almaty, Kazakhstan were studied. Under the conditions of a radiation experiment lasting 21.5 days at a reactor power of 6 MW, lithium ceramics in an argon (Ar) environment were exposed to thermal neutrons with a flux density of  $2\text{E}13 \text{ n}/(\text{cm}^2\cdot\text{s})$ . The temperature of the samples during irradiation did not exceed 320 K. The thermal neutron fluence accumulated as a result of irradiation was  $3.7\text{E}19 \text{ cm}^{-2}$ .

Two-phase lithium ceramics  $\text{Li}_2\text{TiO}_3\text{-Li}_4\text{SiO}_4$  is a material consisting of two different phases:  $\text{Li}_2\text{TiO}_3$  and  $\text{Li}_4\text{SiO}_4$ . These phases have different crystal structures and chemical compositions, which makes them interesting objects to combine with the purpose to keep highest possible content of lithium from LOS and to gain better mechanical strength from LMT [1]. In this work, we studied the single composition 25 %LMT + 75 %LOS.

Pebbles with different compositions were fabricated by a melt-based process at KIT [1] and it was found that there is a eutectic point at about 80/20 mol% LOS/LMT with a melting temperature of approximately 1500 K. A significant increase in the mechanical strength was only obtained beyond the eutectic, i.e., at LMT contents of >20 mol% LMT.

As the irradiated samples diameter ranged from 250 to 1250  $\mu\text{m}$ , four pebbles with approximately the same size and weight were selected to conduct TDS experiments. Before the start of TDS experiments, each pebble was subjected to characterization and weighing. Detailed data on the mass of the samples are presented in Table 1. The exact dimensions of the pebbles were also determined using the ImageJ software [28]. The pebble diameter and the deviation from the average value are given for each pebble.

### Experiments

TDS experiments were carried out on an installation designed for mass spectrometric analysis of gas evolution from irradiated materials in vacuum in real time. Fig. 1 shows a schematic diagram of the installation. The TDS installation includes: vacuum pumping system, measuring

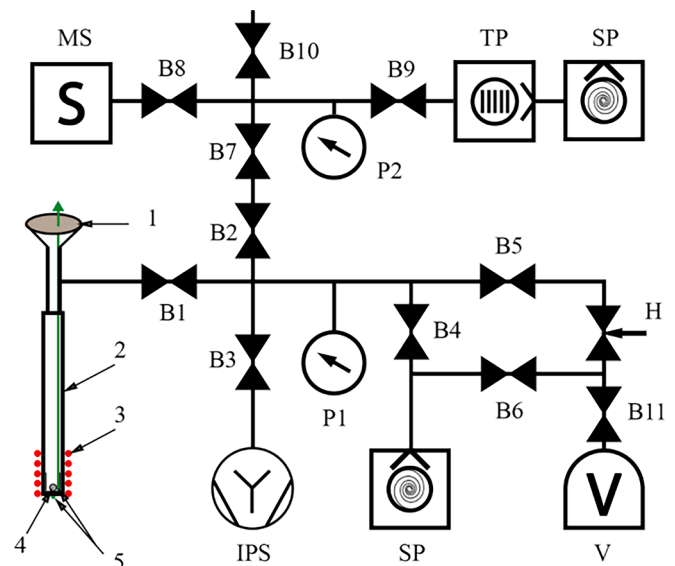


Fig. 1. Thermal desorption mass spectrometry setup. 1 – sealed lead-in; 2 – experimental cell; 3 – heater; 4 – pebble; 5 – thermocouples; P1-P2 – pressure sensors; TP – turbomolecular pump; MS – mass spectrometer; IPS – magnetic discharge pump; SP – dry spiral pump; V – volume with supplied gas; H – precise leak-in.

system and experimental device (ED).

The vacuum pumping system of the installation includes a turbomolecular pump, a magnetic discharge pump and a fore-vacuum pump. When conducting TDS experiments, we used a high-vacuum oil-free pumping post based on a TwisTorr 304 FS turbomolecular pump and an IDP-7 dry spiral pump (Agilent Technologies both), which completely eliminates the possibility of high-molecular organic compounds entering the vacuum system of the installation. The post provides the pump-out rate – 200 l/s and limit vacuum  $10^{-10}$  mbar.

The measurement system of the installation includes a quadrupole mass spectrometer RGA-100 (Stanford Research Systems, USA), temperature and pressure sensors, a multi-channel data-logger, heating control and measuring equipment. Measuring equipment provides control, measurement and recording of parameters during experiments.

The ED consists of: an experimental cell, a sealed lead-in, a heater, thermocouples and a transfer crucible. The capsule is prepared from molybdenum and is attached to an adapter made of stainless steel. The sealed lead-in is designed for installing one thermocouple inside the cell. There is also a second thermocouple at the cell bottom to monitor its external temperature. The geometric dimensions of the experimental device and appearance are shown in Fig. 2.

The procedure for conducting TDS studies was as follows: a single test pebble was placed in a molybdenum transfer crucible, which was then loaded into the experimental cell. The entire system was sealed and pumped out with a turbomolecular pump (TP) to a pressure of about  $10^{-3}$  Pa. Then the heating of the pebble was turned on, and it was linearly

Table 1  
Pebble characteristics.

Pebble	N <sup>o</sup> 1	N <sup>o</sup> 2	N <sup>o</sup> 3	N <sup>o</sup> 4
Weight, mg	1.28 ± 0.02	1.32 ± 0.02	1.28 ± 0.02	1.28 ± 0.02
Diameter, mm	1.17 ± 0.2	1.21 ± 0.4	1.20 ± 0.4	1.18 ± 0.3
Appearance				
	1.5 mm	1.5 mm	1.5 mm	1.5 mm

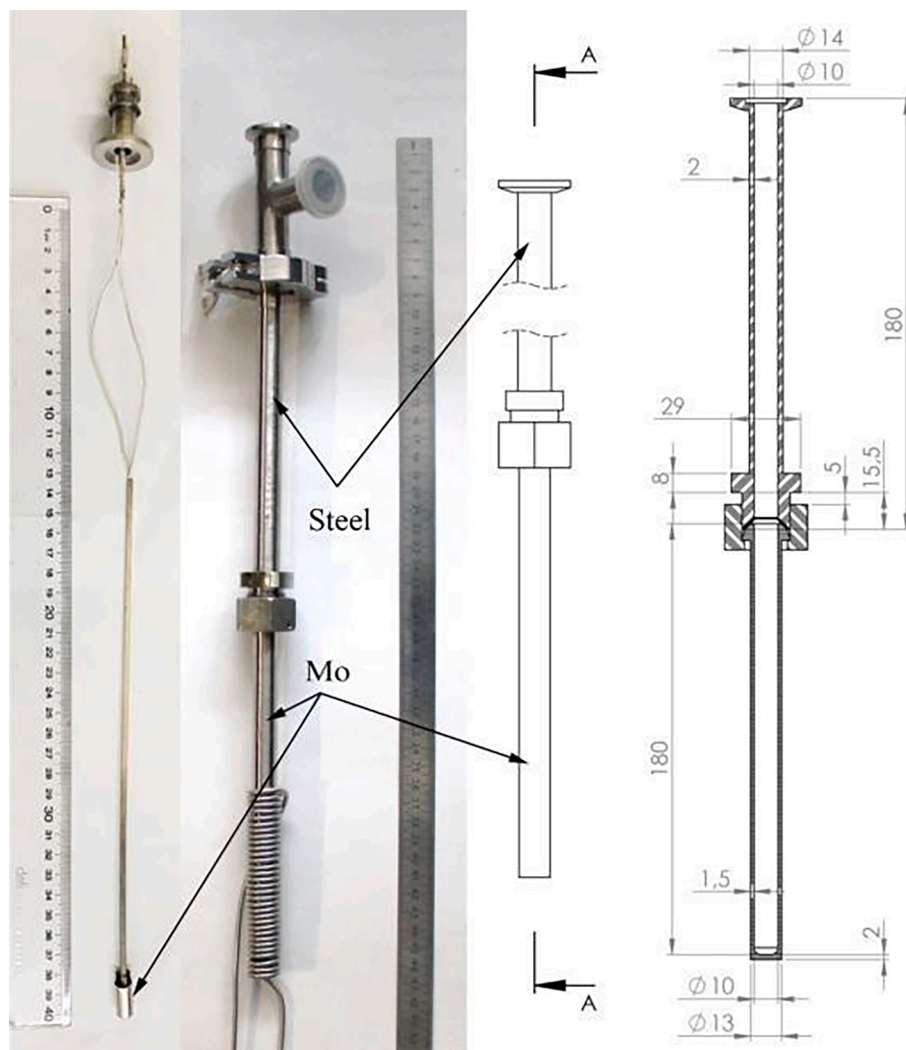


Fig. 2. Appearance and drawing of the experimental device.

heated at a rate of 10 K/min to a temperature of 373 K, and maintained at this temperature for 30 min, this is necessary to reduce the background level of atmospheric gases in the pebble area. Then it was followed by linear heating of the pebble at a rate of 5 K/min or 10 K/min to a temperature of 1173 K, with holding at this temperature for 5 min. After that the pebble was cooled at a rate of 20 K/min. Temperature control was carried out by a PID controller (proportional-integral-differential) using an external thermocouple (T2). Throughout the experiment, a gas mass spectrometer recorded changes in the composition of gases in the experimental cell. When conducting TDS experiments, in addition to mass spectrometric data, changes in temperature from the readings of two thermocouples (T1-T2) and absolute pressure in the installation chamber (P1-P2) were recorded by data-logger.

When conducting the TDS experiments, the following main parameters of the RGA (Residual Gas Analyzer) 100 mass spectrometer were established:

- Detector type: Faraday cup;
- Electron energy: 70 eV;
- Focusing voltage: 50 V;
- Emission current: 0.05 mA;
- Channel Electron Multiplier (CEM): disabled.
- Mass registration range: 1–46 a.m.u.

## Results and discussion

The primary analysis of the obtained mass spectrometer data showed that the main gases for which noticeable changes in partial pressures are observed have the following mass numbers: M2, M3, M4, M6, M12, M14, M16, M17, M18, M19, M20, M22, M28, M32, M40, M44. For further work with mass analysis data and construction of a complete diagram of the temperature dependence of changes in the composition of gases in the working chamber with the sample, the mass numbers given above were considered.

The main and most informative period of these experiments is the area during linear heating of the pebble from 400 K to 1173 K. Therefore, for further discussion of the data obtained, let us present the linear heating area as the temperature dependence of the change in the gas composition in the experimental cell with the samples (see Fig. 3).

Here, let us make a note that the initially obtained mass-spectra require some processing, since the mass spectrometer registers, in addition to the main peak according to the mass number (M) of the gas, a superposition of peaks of other mass numbers (as ionized fragments of a gas molecule with mass number M, and different molecules containing different isotopes of the element included in the gas molecule). This leads to the known fact that for some mass numbers the peaks will be determined by the superposition of different contributions from different gas molecules. Table 2 clearly shows the spectra of gases that correspond to the mass numbers of interest. As can be seen, among the

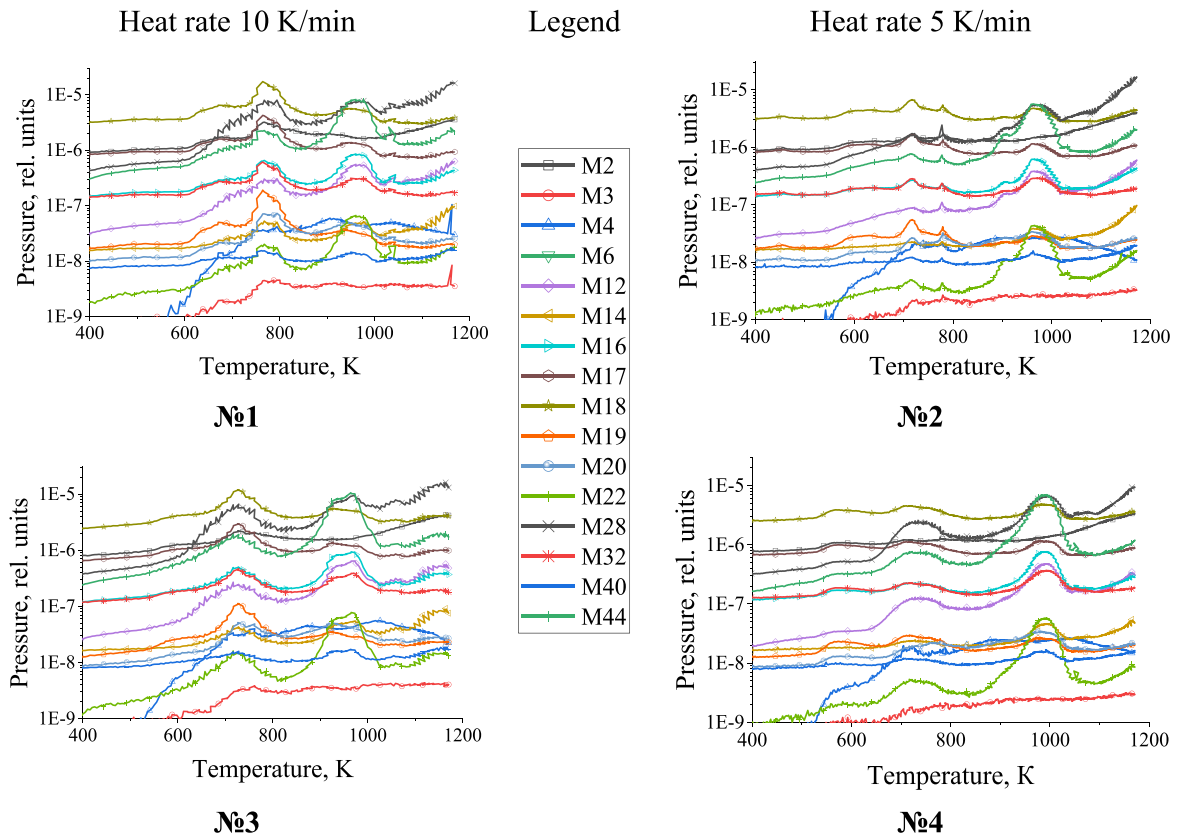


Fig. 3. TDS data. Temperature dependence of changes in partial pressure of gases for samples No. 1–4 in the range from 400 K to 1173 K.

mass numbers of interest, coincidences occur for many other gases.

To decipher the RGA-100 mass spectra and to obtain real values for the gases under study in the chamber, a system of linear equations was solved:

$$M_z = \sum_i \gamma_{z,i} \times M_i \quad (1)$$

where  $M_z$  - peak value in the mass-spectrum for mass number  $z$ ,  $M_i$  - partial pressure of gas  $i$ ,  $\gamma_{z,i}$  - ratio of  $i$  gas in the peak of  $M_z$ .

From the experimental data of TDS experiments it is clear that in addition to tritium-containing gases (HT, T<sub>2</sub>, HTO, T<sub>2</sub>O) and helium (<sup>4</sup>He), there are atmospheric gases (N<sub>2</sub>, O<sub>2</sub>, Ar, CO<sub>2</sub>), water (H<sub>2</sub>O) and hydrogen (H<sub>2</sub>).

We attribute the presence of atmospheric gases and water vapor in the TDS spectra to the fact that after irradiation the samples were removed from sealed cell and left in an open atmospheric environment. As a result, water and atmospheric gases penetrate into the pores and intergranular voids, where they were enclosed in various kinds of traps (V1-V3). Additionally, filling with atmospheric gases occurred.

Next, let us consider the gas evolution of water vapor. The mass spectrum of water is decomposed into the following ions: H<sub>2</sub>O (M18), HO (M17), O (M16), H<sub>2</sub><sup>17</sup>O (M19), H<sub>2</sub><sup>18</sup>O (M20). Let us consider separately the changes in pressure during TDS for these mass numbers, see Fig. 4.

It can be seen that pressure changes for gases with mass numbers M18, M17, M19 have the same kinetics. The difference for gases with mass number M16 is easily explained by the large number of overlaps from different gases according to Table 2. For gases with mass number M20, a significant portion of the contribution to the peak is determined by the water isotope H<sub>2</sub><sup>18</sup>O (natural), against which the contribution for the HTO molecule is difficult to determine. The same situation occurs when assessing the release of tritium water (T<sub>2</sub>O - M22). Here the main contribution to the peak is the doubly ionized CO<sub>2</sub><sup>++</sup> molecule. Anyway,

the magnitudes of these peaks are significantly smaller than the peak of tritium release in the form of an HT molecule and may not be taken into account in the balance of released tritium. The data on the content of water and HT molecule in the gas composition obtained in our study agree with the results of the work published in the Journal of Nuclear Materials [29]. This confirms that the influence of humidity on the chemical composition and temperature characteristics of hydrogen isotope release plays a key role in the processes related to tritium control.

The obtained results of the TDS spectra can be explained by complex sorption-desorption processes and chemical reactions occurring both on the surface of the sample and on the walls of the working chamber and crucible. The complexity is further compounded by the presence of numerous atmospheric gases and water vapor that interacted with the surfaces of the samples both before and after the irradiation experiments, despite the fact that the irradiations were carried out in an argon atmosphere. The schematic diagram below illustrates the primary reactions (see Fig. 5), which will be discussed in more detail later.

If we divide the mechanisms of gas release according to the temperature scale, we can distinguish four characteristic zones with regard to the release and processes on surfaces.

*The first zone*, covering the temperature range from 400 K to 500 K, determines the background level of gases in the chamber with the sample. This background is due to the release and migration of water and atmospheric gases from open pores and defects of the pebble (traps of the first type in the figure are indicated as V1).

*In the second zone*, some activation of the pebble surface occurs (500 K-550 K).

We believe that initially the surface of the irradiated samples is depleted in oxygen and has a dark tint (see Table 3). Oxygen vacancies on this surface can interact with various elements:

**Table 2**  
Interpretation of the RGA mass spectrum for TDS experiments.

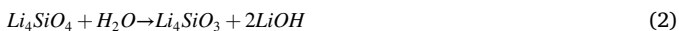
Gas, i	Hydrogen gas with various isotopes		Helium	Water with various hydrogen and oxygen isotopes			Carbon monoxide	Nitrogen	Oxygen	Argon	Carbon dioxide
M, z											
2	H <sub>2</sub>										
3		T	T								
4		HT		<sup>4</sup> He							
6			T <sub>2</sub>								
12							C				C
14							CO <sup>++</sup>	N <sub>2</sub> <sup>++</sup>			
16				O	O	O	O		O		O
17				HO	HO						
18				H <sub>2</sub> O							
19				H <sub>2</sub> <sup>17</sup> O	TO	TO					
20				H <sub>2</sub> <sup>18</sup> O	HTO					Ar <sup>++</sup>	
22						T <sub>2</sub> O					CO <sub>2</sub> <sup>++</sup>
28							CO	N <sub>2</sub>			CO
32									O <sub>2</sub>		
40										Ar	
44											CO <sub>2</sub>

<sup>++</sup> – doubly ionized gas

<sup>++</sup> – doubly ionized gas.

- Interaction with H<sub>2</sub>O: Water molecules in contact with the surface can form O–H complexes, leaving free hydrogen atoms on the surface of the sample (a reversible process).
- Interaction with CO<sub>2</sub>: Carbon dioxide molecules reaching the surface from the gas phase can form O–C complexes, leaving free oxygen atoms on the surface of the sample. The O–C complexes are then desorbed from the surface, forming carbon monoxide gas.

In addition, H<sub>2</sub>O can undergo reactions with Li<sub>4</sub>SiO<sub>4</sub>.



Associated H<sub>2</sub> molecules can also undergo reactions with Li<sub>4</sub>SiO<sub>4</sub>.



In the second stage, LiOH reacts with CO<sub>2</sub>, forming Li<sub>2</sub>CO<sub>3</sub> [30].



H<sub>2</sub> molecules falling on the surface can dissociate into individual atoms. Free tritium atoms are delivered to the surface of the ceramic from the bulk due to the processes of diffusion and mass-transfer. Considering that the number of free hydrogen atoms is several orders of magnitude greater than the number of tritium atoms, the desorption process turns out to be much “faster” compared to the speed of tritium delivery to the surface. As a result, tritium atoms associate with hydrogen atoms and are desorbed in the form of an HT molecule.

The HT release front is observed at temperatures of about 550 K, which is almost the same for all four experiments and is characterized by rapid desorption of tritium from the sample surface (Peak 1). Further, it is in this zone that water and atmospheric gases have a high peak of release, which is associated with the opening of traps of the second type

(V2). After this, due to the increase in the surface of the sample, Peak 2 of HT release occurs (see Fig. 7).

The third zone starts from 800 K to 850 K, where, as we believe, the surface of the sample replenishes the oxygen balance and acquires a natural white tint (see Table 3).

In this zone, water and atmospheric gases give a second peak of release, associated with the exit from traps of the third type (V3). The peak of atmospheric gases is followed by a third peak of HT release, associated with the exposure of additional surfaces.

The observed intense release of CO<sub>2</sub> may be a consequence of reactions of Li<sub>2</sub>CO<sub>3</sub> with Li<sub>2</sub>SiO<sub>3</sub> accumulated in the surface layer [11,31].



Immediately after the decrease in the CO<sub>2</sub> level in the chamber with the sample, due to the restoration of the sample surface by Li<sub>4</sub>SiO<sub>4</sub>, the release of hydrogen tends to approach the Peak 3.

In the fourth zone, the most significant increase is observed for the release of CO gas. This is due to the heating of the stainless-steel walls (the upper part of the experimental cell), where CO and H<sub>2</sub> are actively produced. The partial pressure of H<sub>2</sub> (M2) also has a significant increase in this area. Experiments conducted with the crucible without a sample showed comparable values for the gas data in Zone 4.

It is also worth emphasizing that our measurements of the mass of samples before and after TDS experiments showed that, despite the noticeable release of gases, mass losses were insignificant and did not exceed the limits of the measurement error of the equipment used.

### Analysis of results

According to the obtained TDS data and the conclusion made in the previous section, we can conclude that all tritium is predominantly

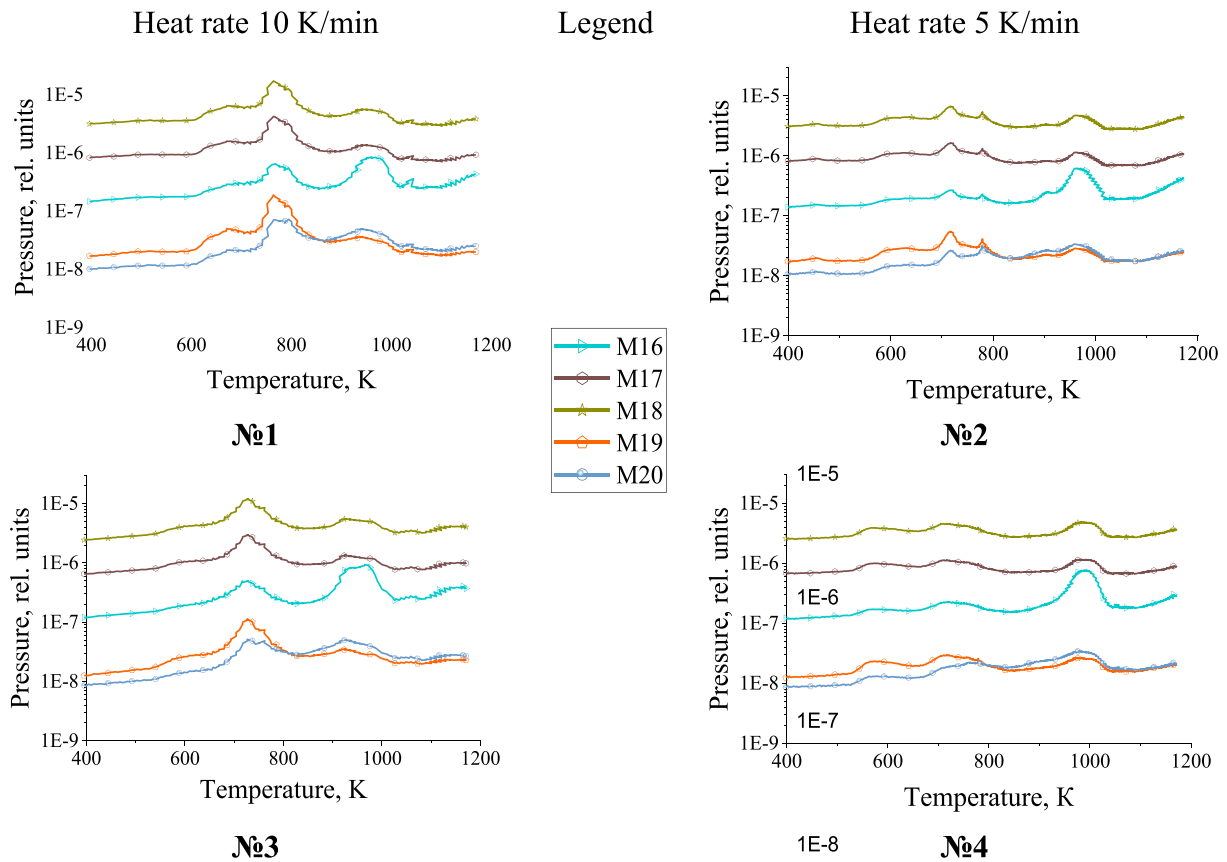


Fig. 4. Temperature dependence of changes in partial pressure of water in the range from 400 K to 1173 K.

located in two main components present in the mass spectrum: M3 (T) and M4 ( ${}^4\text{He} + \text{HT}$ ), the release of tritium in the form of a molecule  $\text{T}_2$  (M6) not visible. We here assume, based on our experience conducting TDS experiments with LMT ( $\text{Li}_2\text{TiO}_3$ ) samples [32], that the release of accumulated helium in such experiments occurs at temperatures exceeding 1300 K and is complete only at temperatures close to the melting point.

As for the change in pressure for peak M3, it is initially determined by the pressure of the neighboring peak M2, this can be seen from the diagram (see Fig. 6), but a simultaneous further increase in the partial pressure of peaks M3 and M4 suggests that this is still a peak of the ionized tritium atom. Nevertheless, the influence of  $\text{H}_2$  on M3 remains dominant, since the level of M2 is 100 times higher than the level of M4 and M3 in the experiment, and an attempt to include T (M3) in the balance leads to significant errors.

To assess the release of tritium-containing gases, let us consider the release of HT. From the results presented in Table 4, it follows that a decrease in heating rate causes a shift of all peaks toward lower temperatures, which corresponds to typical RTD dependences in various models. This shift is explained by the change in desorption kinetics at different heating rates. This is especially true for the first peak, whose shift depends to a greater extent on the surface condition of the sample, indicating a significant influence of surface processes on tritium desorption. Differences in peak displacement between samples heated at the same rate can be related to the variety of structural and geometric characteristics of the samples. The release front is clearly visible in the summary Fig. 7, which is rapidly growing in the first peak zone. Here, the main contribution comes from free tritium atoms already deposited on the surface and subsurface layers of the ceramic sample.

Then, in the zone of the second peak, HT are intensively desorbed from the cleaned surface of the sample, due to the release from traps of the second type (V2). In the region of peak reduction, additional surfaces

are opened due to the release of traps of the third type (V3), as a result of which the third peak appeared.

Based on the obtained TDS dependences, the integral amounts of released tritium from irradiated lithium ceramic samples were estimated, which coincided well with each other (see Table 5). In addition, using the developed model of the WWR-K core and irradiator, as well as MCNP software for particle transport analysis, the prediction of tritium formation in the  ${}^6\text{Li} (n,\alpha)\text{T}$  reaction in two-phase lithium ceramics was carried out. Theoretical calculations based on the density ( $2.84 \text{ g/cm}^3$ ) and total volume of irradiated samples ( $0.20 \text{ cm}^3$ ), as well as the reaction rate ( $2.16\text{E}13 \text{ reactions/cm}^3\cdot\text{s}$ ), suggested tritium formation in the ceramics of approximately  $6.8\text{E}-4 \text{ mol/cm}^3$  in 21.5 days. Comparison of the theoretical calculations with the experimentally determined values of the total amount of released tritium showed a good order of magnitude match.

The resulting TDS curves can be described by three desorption peaks of tritium yield from traps of limited capacity (V1-V3) of the following form  $dC_i/dt = -rate_i (C_i - C_{i0})$  ( $C_i$  – the surface concentration of tritium atoms), where,  $rate_i = k_{des} \times C_i \times q_i$ . Then the desorption coefficient may be the same for all peaks and was defined as:

$$k_{des} [\text{s}^{-1}] = 300 \times \exp\left(\frac{-1.45 [eV]}{k_B T}\right) \quad (6)$$

The obtained values of the parameters of the tritium release gas constant for sample 3 (second peak) were compared with the data for the detrapping rate constant [6] (see Table 6). Small differences may be due to the specifics of our samples, such as microstructure or composition, as well as to the experimental conditions.

Next, the values of  $q_i$  and the initial concentrations of tritium in traps  $C_{i0}$  were selected (see Table 7). An example of the simulated curve for sample 3–4 is shown in Fig. 7.

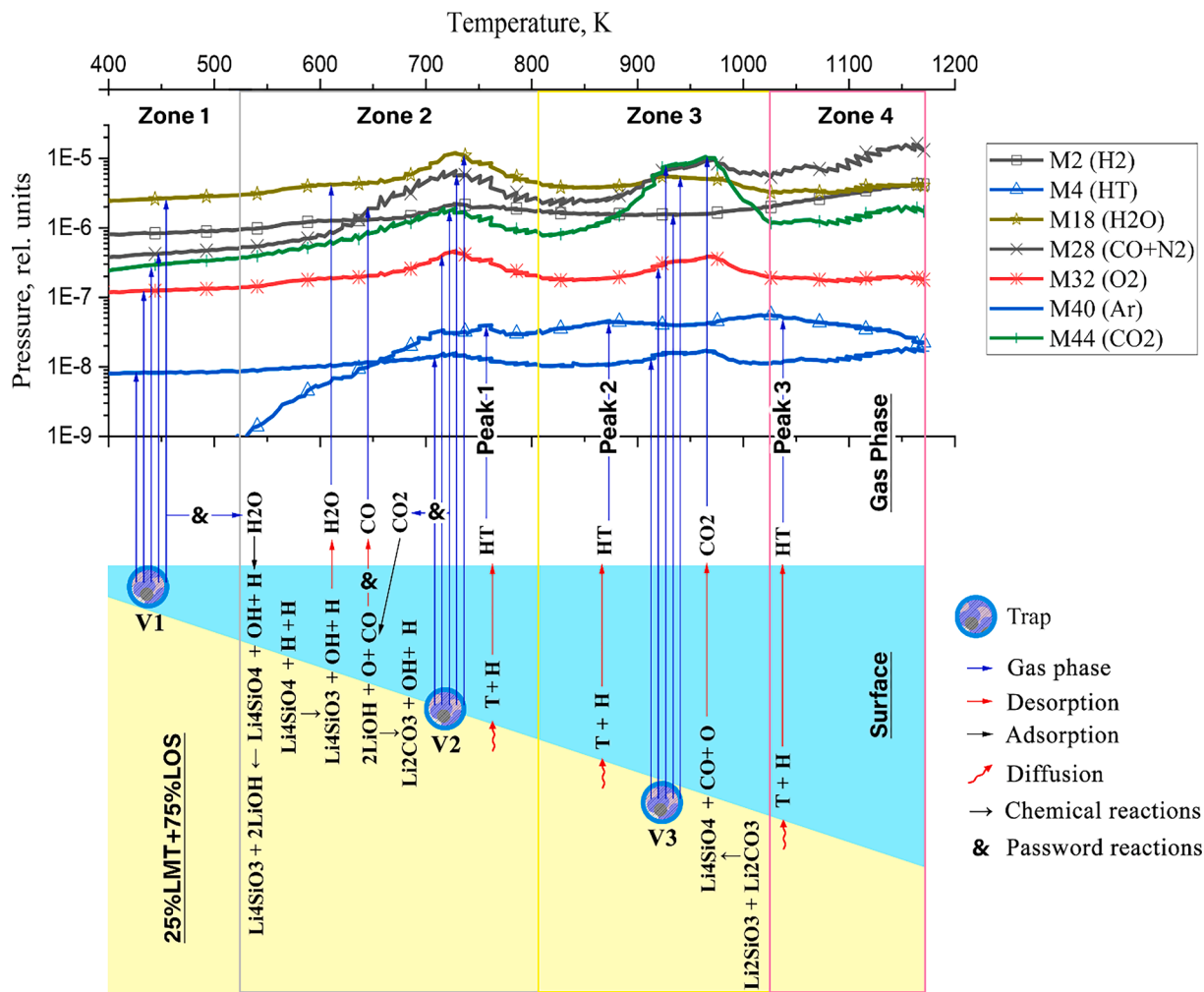


Fig. 5. Schematic illustration of the main processes in a cell with a sample of irradiated two-phase lithium ceramics using the example of the results of an experiment with pebble N<sup>o</sup>3.

Table 3

Changes in the appearance of irradiated pebble N<sup>o</sup>1 before and after TDS experiment.

Pebble N <sup>o</sup> 1	
Before TDS	After TDS
	
1.5 mm	1.5 mm

### Conclusion

Studies using the method of thermal desorption spectroscopy on irradiated two-phase lithium ceramics 25 mol% Li<sub>2</sub>TiO<sub>3</sub> + 75 mol% Li<sub>4</sub>SiO<sub>4</sub> made it possible to qualitatively describe the processes of tritium release and to propose a reasonable mechanism for the release of tritium from samples when they are linearly heated to 1173 K. This mechanism can be formulated as follows:

- The release of tritium is predominantly desorption in nature. This means that tritium is released from the samples as a result of desorption from the outer and inner surfaces of the material.

- Most of the released tritium comes out as HT molecules. This is due to the presence of a significant amount of water molecules (H<sub>2</sub>O) and, therefore, hydrogen molecules (H<sub>2</sub>) in the sample chamber.
- Experiments have shown that the main amount of tritium is evenly distributed throughout the ceramic volume. Its output is determined by transfer from voids and traps to the boundaries that communicate with the outer surface of the ceramic. The kinetics of tritium release depends on the number, size and depth of the exit paths of such areas inside the ceramic.
- Based on the analysis of TDS dependences, the integral amounts of released tritium from irradiated lithium ceramic samples were estimated, and these estimates correlate well with each other.
- Simulation made it possible to determine the temperature dependence of the tritium desorption coefficient in irradiated two-phase lithium ceramics and to estimate capacities of main traps.
- As for helium, it is assumed that the main amount of helium is retained in the volume of ceramics up to temperatures close to the melting point.

These results and the mechanism of tritium release during linear heating of lithium ceramic samples may be important for understanding the behavior of materials in fusion reactors and contribute to the further development of nuclear energy.

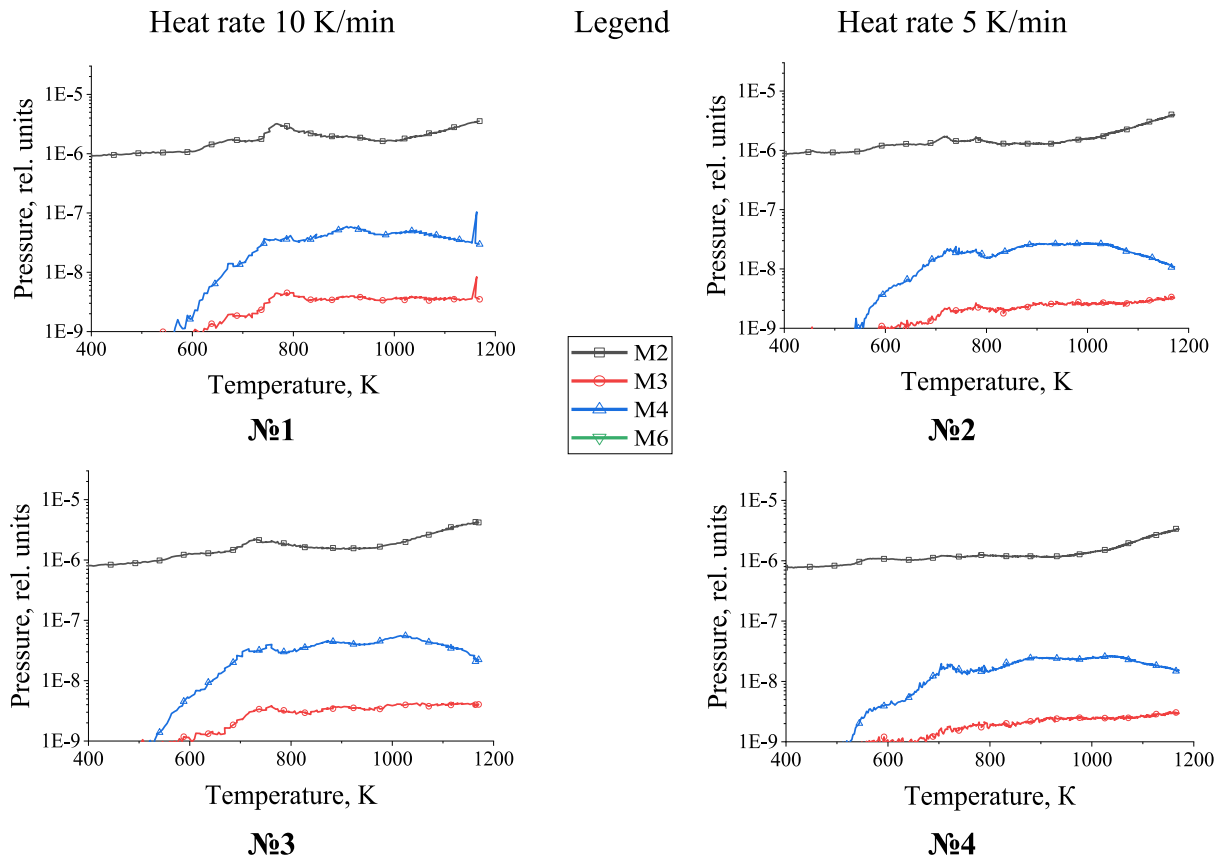


Fig. 6. Temperature dependence of the change in pressure of gases H<sub>2</sub>, HT, T<sub>2</sub> in the range from 400 K to 1173 K.

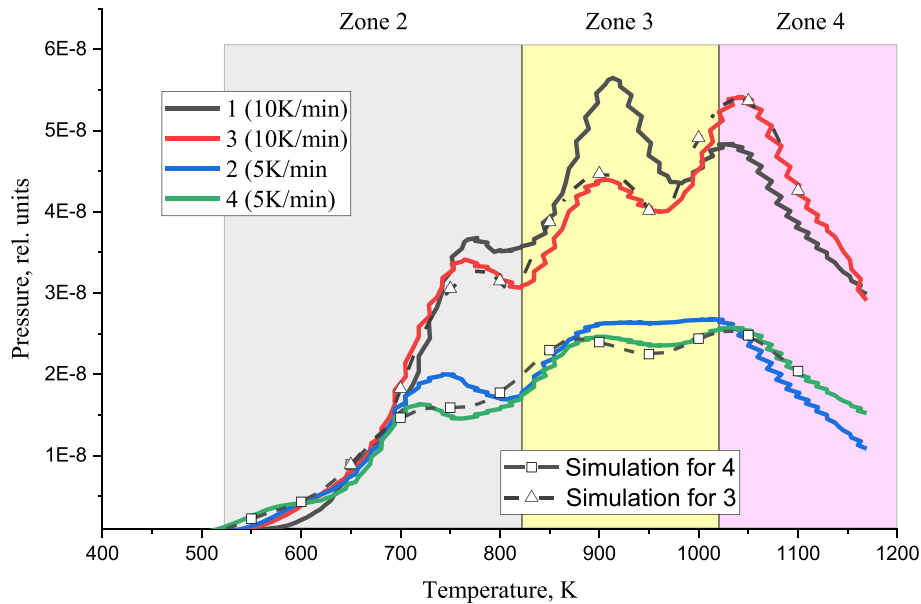


Fig. 7. Summary chart of HT release for all 4 TDS experiments.

**Funding**

The research has been funded by the Committee of Science of the Ministry of Science and Higher Education of the Republic of Kazakhstan with Grant No. AP13068172.

**CRediT authorship contribution statement**

**Yevgen Chikhray:** Conceptualization, Investigation, Writing – original draft. **Saulet Askerbekov:** Conceptualization, Investigation, Writing – original draft. **Regina Knitter:** Resources. **Timur Kulsartov:** Conceptualization, Investigation, Writing – original draft. **Asset Shaimerdenov:** Investigation, Project administration, Writing – review &

**Table 4**

Summary table of tritium molecule release peaks.

Pebble			Peak 1	Peak 2	Peak 3
N <sup>2</sup> 1	Heat rate	Position, K	767	913	1039
	10 K/min	Height, arb. units	3.64E-08	5.65E-08	4.83E-08
N <sup>2</sup> 3	_____	Position, K	766	909	1034
	_____	Height, arb. units	3.40E-08	4.38E-08	5.41E-08
N <sup>2</sup> 2	Heat rate	Position, K	743	901	1012
	5 K/min	Height, arb. units	2.07E-08	2.63E-08	2.67E-08
N <sup>2</sup> 4	_____	Position, K	722	892	1029
	_____	Height, arb. units	1.76E-08	2.47E-08	2.60E-08

**Table 5**

Amounts of released tritium from irradiated lithium ceramic samples.

Sample	Amount, mole
N <sup>2</sup> 1	4.93E-08
N <sup>2</sup> 2	5.34E-08
N <sup>2</sup> 3	4.89E-08
N <sup>2</sup> 4	5.22E-08

**Table 6**

Comparison of desorption constant parameters.

Parameter/Data source	Experimental data for Sample 3 (Peak 2)	Literature data
Activation energy [eV]	1.45 ± 0.02	1.41
Pre-exponential factor [s <sup>-1</sup> ]	1.8E4 ± 200	1.5E4

**Table 7**

Simulation parameters.

Peak	Sample 4 (5 K/min)		Sample 3 (10 K/min)	
	q <sub>i</sub>	C <sub>i,0</sub> , mol/cm <sup>2</sup>	q <sub>i</sub>	C <sub>i,0</sub> , mol/cm <sup>2</sup>
1	600	1E-7	2200	1.1E-7
2	40	2.2E-7	90	2.2E-7
3	6	5.5E-7	9	5.6E-7

editing. **Magzhan Aitkulov:** Formal analysis, Investigation. **Assyl Akhanov:** Investigation, Methodology. **Darkhan Sairanbayev:** Investigation, Software. **Zhanar Bugybay:** Formal analysis, Visualization. **Aigerim Nessipbay:** Formal analysis, Software. **Kirill Kisselyov:** Software, Visualization. **Gunta Kizane:** Conceptualization. **Arturs Zarins:** Formal analysis.

### Declaration of competing interest

The authors declare that they have no known competing financial interests or personal relationships that could have appeared to influence the work reported in this paper.

### Data availability

The authors do not have permission to share data.

### References

- R. Knitter, M.H.H. Kolb, U. Kaufmann, A.A. Goraieb, Fabrication of modified lithium orthosilicate pebbles by addition of titania, *J. Nucl. Mater.* 442 (1–3) (2013) S433–S436, <https://doi.org/10.1016/j.jnucmat.2012.10.034>.
- M.H.H. Kolb, R. Knitter, T. Hoshino, Li<sub>4</sub>SiO<sub>4</sub> based breeder ceramics with Li<sub>2</sub>TiO<sub>3</sub>, LiAlO<sub>2</sub> and LiXLaYTiO<sub>3</sub> additions, part II: Pebble properties, *Fusion Eng. Des.* 115 (2017) 6–16, <https://doi.org/10.1016/j.fusengdes.2016.12.038>.
- G.J. Rao, R. Mazumder, S. Bhattacharyya, P. Chaudhuri, Fabrication and characterization of Li<sub>4</sub>SiO<sub>4</sub>-Li<sub>2</sub>TiO<sub>3</sub> composite ceramic pebbles using extrusion and spheroidization technique, *J. Eur. Ceram. Soc.* 38 (15) (2018) 5174–5183, <https://doi.org/10.1016/j.jeurceramsoc.2018.07.018>.
- C. Dang, M. Yang, Y.C. Gong, L. Feng, H.L. Wang, Y.L. Shi, Q.W. Shi, J.Q. Qi, T. C. Lu, A promising tritium breeding material: Nanostructured 2Li<sub>2</sub>TiO<sub>3</sub>-Li<sub>4</sub>SiO<sub>4</sub> biphasic ceramic pebbles, *J. Nucl. Mater.* 500 (2018) 265–269, <https://doi.org/10.1016/j.jnucmat.2018.01.010>.
- M. Yang, Y.C. Gong, G.M. Ran, H.L. Wang, R.C. Chen, Z.Y. Huang, Q.W. Shi, X. J. Chen, T.C. Lu, C.J. Xiao, Tritium release behavior of Li<sub>4</sub>SiO<sub>4</sub> and Li<sub>4</sub>SiO<sub>4</sub> + 5 mol% TiO<sub>2</sub> ceramic pebbles with small grain size, *J. Nucl. Mater.* 514 (2019) 284–289, <https://doi.org/10.1016/j.jnucmat.2018.12.013>.
- Q.L. Zhou, A. Togari, M. Nakata, M.Z. Zhao, F. Sun, Q. Xu, Y. Oya, Release kinetics of tritium generation in neutron irradiated biphasic Li<sub>2</sub>TiO<sub>3</sub>-Li<sub>4</sub>SiO<sub>4</sub> ceramic breeder, *J. Nucl. Mater.* 522 (2019) 286–293, <https://doi.org/10.1016/j.jnucmat.2019.05.033>.
- S. Hirata, K. Ashizawa, F. Sun, Y.J. Feng, X.Y. Wang, H.L. Wang, M. Kobayashi, A. Taguchi, Y. Oya, Tritium recovery behavior for tritium breeder Li<sub>4</sub>SiO<sub>4</sub>-Li<sub>2</sub>TiO<sub>3</sub> biphasic material //, *J. Nucl. Mater.* 567 (2022), <https://doi.org/10.1016/j.jnucmat.2022.153838>.
- I. Kenzhina, T. Kulsartov, R. Knitter, Y. Chikhray, Y. Kenzhin, Z. Zaurbekova, A. Shaimerdenov, G. Kizane, A. Zarins, A. Kozlovskiy, M. Gabdullin, A. Tolonova, E. Nesterov, Analysis of the reactor experiments results on the study of gas evolution from two-phase Li<sub>2</sub>TiO<sub>3</sub>-Li<sub>4</sub>SiO<sub>4</sub> lithium ceramics, *Nucl. Mater. Energy.* 30 (2022), <https://doi.org/10.1016/j.nme.2022.101132>.
- T. Kulsartov, Z. Zaurbekova, R. Knitter, A. Shaimerdenov, Y. Chikhray, S. Askerbekov, A. Akhanov, I. Kenzhina, G. Kizane, Y. Kenzhin, M. Aitkulov, D. Sairanbayev, Y. Gordienko, Y. Ponkratov, Studies of two-phase lithium ceramics Li<sub>4</sub>SiO<sub>4</sub>-Li<sub>2</sub>TiO<sub>3</sub> under conditions of neutron irradiation, *Nucl. Mater. Energy.* 30 (2022), <https://doi.org/10.1016/j.nme.2022.101129>.
- Y. Chikhray, V. Shestakov, O. Maksimkin, L. Turubarova, I. Osipov, T. Kulsartov, K. Tsuchiya, Study of Li<sub>2</sub>TiO<sub>3</sub>+5mol% TiO<sub>2</sub> lithium ceramics after long-term neutron irradiation, *J. Nucl. Mater.* 386–388 (2009) 286–289, <https://doi.org/10.1016/j.jnucmat.2008.12.111>.
- T. Kulsartov, I. Kenzhina, Ye. Chikhray, et al., Determination of the activation energy of tritium diffusion in ceramic breeders by reactor power variation, *Fusion Eng. Des.* 172 (2021), <https://doi.org/10.1016/j.fusengdes.2021.112783>.
- T. Kulsartov, A. Shaimerdenov, Z.h. Zaurbekova, et al., Features of the in-situ experiments on studying of tritium release from lithium ceramic Li<sub>2</sub>TiO<sub>3</sub> using vacuum extraction method, *Fusion Eng. Des.* 172 (2021), <https://doi.org/10.1016/j.fusengdes.2021.112703>.
- T. Kulsartov, Z. Zaurbekova, R. Knitter, I. Kenzhina, Y. Chikhray, A. Shaimerdenov, S. Askerbekov, G. Kizane, A. Yelishenkov, T. Zholdybayev, Comparative analysis of gas release from biphasic lithium ceramics pebble beds of various pebbles sizes and content under neutron irradiation conditions, *Nucl. Mater. Energy* 38 (2024), <https://doi.org/10.1016/j.nme.2024.101583>.
- N.V. Larionova, P.Y. Krivitskiy, A.V. Toporova, Y.N. Polivkina, A.O. Aidarkhanov, ACCUMULATION OF CS-137 AND SR-90 BY PLANTS IN THE FALLOUT AREA AT THE SEMIPALATINSK TEST SITE, *NNC RK Bulletin* (2022), <https://doi.org/10.52676/1729-7885-2022-3-26-30>.
- P.Y. Krivitskiy, Peculiarities of radioactive soil contamination in places of underground nuclear tests in the Semipalatinsk test site, *J. Environ. Radioact.* (2022), <https://doi.org/10.1016/j.jenvrad.2022.106991>.
- A.Y. Kunduzbayeva, Speciation of <sup>137</sup>Cs, <sup>90</sup>Sr, <sup>241</sup>Am, and <sup>239+240</sup>Pu artificial radionuclides in soils at the Semipalatinsk test site, *J. Environ. Radioact.* (2022), <https://doi.org/10.1016/j.jenvrad.2022.106867>.
- B. Chektybayev, A. Sadykov, E. Batyrbekov, M. Skakov, D. Zarva, I. Tazhibayeva, V. Pavlov, Study of breakdown and plasma formation in the KTM tokamak with the massive conductive vacuum chamber, *Fusion Eng. Des.* 163 (2021) 112167, <https://doi.org/10.1016/j.fusengdes.2020.1121>.
- Tazhibayeva, et al., Material science activities for fusion reactors in Kazakhstan, *J. Nucl. Mater.* (2009), <https://doi.org/10.1016/j.jnucmat.2008.12.111>.
- E. Batyrbekov, B. Chektybayev, A. Sadykov, M. Skakov, E. Kashikbayev, D. Olkhovik, S. Zhunisbek, Test Results of Active Thermography Method for Plasma-Wall Interaction Studies on the KTM Tokamak, *Fusion Eng. Des.* 161 (2020) 112014, <https://doi.org/10.1016/j.fusengdes.2020.1120>.
- I. Tazhibayeva, M. Skakov, V. Baklanov, E. Koyanbayev, A. Miniyaev, T. Kulsartov, E. Nesterov, Study of properties of tungsten irradiated in hydrogen atmosphere, *Nucl. Fusion* 57 (12) (2017) 126062, <https://doi.org/10.1088/1741-4326/aa7911>.
- M. Skakov, E. Batyrbekov, I. Sokolov, A. Miniyaev, T. Tulenbergenov, Y. Sapataev, N. Orazgaliyev, O. Bukina, G. Zhanbolatova, Y. Kozhakhmetov, Influence of Hydrogen Plasma on the Surface Structure of Beryllium, *Materials* 15 (2022) 6340.
- I. Manika, et al., Effect of ion-induced nuclear reactions on structure modification and radiolysis in LiF irradiated by 410 MeV <sup>36</sup>S ions, *Opt. Mater.* 138 (2023) 113686.
- H. Katsui, et al., Study on compatibility between silicon carbide and solid breeding materials under neutron irradiation, *Fusion Sci. Technol.* 60 (1) (2011) 288–291.
- T. Krasta, et al., Effect of ion-induced secondary radiations on the formation of extended defects and radiolysis beyond the range of swift <sup>12</sup>C, <sup>50</sup>Ti, and <sup>52</sup>Cr ions in LiF, *Nucl. Instrum. Methods Phys. Res., Sect. B* 545 (2023) 165142.
- A. Devaraj, B. Matthews, B. Arey, L. Bagaasen, E. Buck, G. Sevigny, D. Senor, Neutron irradiation induced changes in isotopic abundance of <sup>6</sup>Li and <sup>3</sup>D nanoscale distribution of tritium in LiAlO<sub>2</sub> pellets analyzed by atom probe tomography, *Mater. Charact.* 176 (2021) 111095.
- Q. Qi, J. Wang, Q.L. Zhou, Y.C. Zhang, M.Z. Zhao, S.X. Gu, G.N. Luo, Comparison of tritium release behavior in Li<sub>2</sub>TiO<sub>3</sub> and promising core-shell Li<sub>2</sub>TiO<sub>3</sub>-Li<sub>4</sub>SiO<sub>4</sub>

- biphasic ceramic pebbles, *J. Nucl. Mater.* 539 (2020), <https://doi.org/10.1016/j.jnucmat.2020.152330>.
- [27] M. Yang, L.J. Zhao, Y. Qin, G.M. Ran, Y. Gong, H.Y. Wang, T.C. Lu, Tritium release property of Li<sub>2</sub>TiO<sub>3</sub>-Li<sub>4</sub>SiO<sub>4</sub> biphasic ceramics, *J. Nucl. Mater.* 538 (2020), <https://doi.org/10.1016/j.jnucmat.2020.152268>.
- [28] W.S. Rasband, ImageJ, U. S. National Institutes of Health, Bethesda, Maryland, USA, <https://imagej.nih.gov/ij/>, 1997-2018.
- [29] F.Y. Li, X.Y. Yan, X.J. Deng, Y.X. Yan, M.J. Hu, J.W. Ba, T. Tang, Effect of ambient humidity on deuterium release behavior in Li<sub>4</sub>SiO<sub>4</sub> solid breeder, *J. Nucl. Mater.* 556 (2021), <https://doi.org/10.1016/j.jnucmat.2021.153202>.
- [30] J. Ortiz-Landeros, L. Martínez-dlCruz, C. Gómez-Yáñez, H. Pfeiffer, Towards understanding the thermoanalysis of water sorption on lithium orthosilicate (Li<sub>4</sub>SiO<sub>4</sub>), *Thermochim. Acta* 515 (2011) 73–78, <https://doi.org/10.1016/j.tca.2010.12.025>.
- [31] S.M. Amorim, M.D. Domenico, T.L.P. Dantas, H.J. José, R.F.P.M. Moreira, Lithium orthosilicate for CO<sub>2</sub> capture with high regeneration capacity: kinetic study and modeling of carbonation and decarbonation reactions, *Chem. Eng. J.* 283 (2016) 388–396, <https://doi.org/10.1016/j.cej.2015.07.083>.
- [32] T. Kulsartov, Y. Ponkratov, Z. Zaurbekova, Y. Gordienko, I. Tazhibayeva, I. Kenzhina, K. Samarkhanov, Y. Tulubayev, A. Shaimerdenov, S. Udartsev, Thermal desorption of tritium and helium from lithium ceramics Li<sub>2</sub>TiO<sub>3</sub> + 5 mol % TiO<sub>2</sub> after neutron irradiation, *J. Nucl. Mater.* 585 (2023), <https://doi.org/10.1016/j.jnucmat.2023.154609>.